Allosterically driven self-assemblies of interlocked calix[6]arene receptors

Stéphane Le Gac,* Jean-François Picron, Olivia Reinaud and Ivan Jabin*

Supporting information

Content

Figure S1. ^{1}H NMR spectrum ($CDCl_3$, 328 K, 400 MHz) of **7**.

Figure S2. ^{13}C NMR spectrum ($CDCl_3$, 328 K, 100 MHz) of **7**.

Figure S3. 2D NMR COSY spectrum ($CDCl_3$, 328 K) of **7**.

Figure S4. 2D NMR HMBC spectrum ($CDCl_3$, 328 K) of **7**.

Figure S5. 2D NMR HSQC spectrum ($CDCl_3$, 328 K) of **7**.

Figure S6. ^{1}H NMR spectrum (DMSO-d_6, 373 K, 400 MHz) of **8**.

Figure S7. ^{13}C NMR spectrum (DMSO-d_6, 373 K, 100 MHz) of **8**.

Figure S8. 2D NMR COSY spectrum (DMSO-d_6, 373 K) of **8**.

Figure S9. 2D NMR HMBC spectrum (DMSO-d_6, 373 K) of **8**.

Figure S10. 2D NMR HSQC spectrum (DMSO-d_6, 373 K) of **8**.

Figure S11. ^{1}H NMR spectra ($CDCl_3$, 298 K) of the host-guest complexes $\mathbf{3}_{IMI}^{3H+,3TFA-}$ and $\mathbf{4}_{PrNH3+}^{-6H+,5PrNH3+}$.

Figure S12. 2D NMR HMQC spectrum (2:1 $CD_3OD/CDCl_3$ solution, 298 K) of the host-guest complex $\mathbf{8}_{DopaNH3+}^{-6H+,5DopaNH3+}$.

Figure S13. ^{1}H NMR spectra (2:1 $CD_3OD/CDCl_3$ solution, 298 K) of the host-guest complex $\mathbf{8}_{TryptMeNH3+}^{-6H+,5tBuNH3+}$.

Figure S14. ^{1}H NMR spectra ($CDCl_3$) of $\mathbf{1}_{IMI}^{3H+} \bullet \mathbf{5}_{PrNH3+}^{-3H+}$,**Pic**$^-$, of $\mathbf{1}_{IMI}^{3H+} \bullet \mathbf{5}_{PhCH2CH2NH3+}^{-3H+}$,**Pic**$^-$ and of the assembly $\mathbf{1}_{IMI}^{3H+} \bullet \mathbf{5}_{DopaMe2NH3+}^{-4H+}$.

Figure S15. 2D NMR COSY spectrum ($CDCl_3$, 298 K, selected area) of $\mathbf{1}_{IMI}^{3H+} \bullet \mathbf{5}_{PhCH2CH2NH3+}^{-3H+}$,**Pic**$^-$.

Figure S16. 2D NMR HMQC spectrum ($CDCl_3$, 298 K) of $\mathbf{1}_{IMI}^{3H+} \bullet \mathbf{5}_{PhCH2CH2NH3+}^{-3H+}$,**Pic**$^-$.

Figure S17. 2D NMR COSY spectrum ($CDCl_3$, 298 K, selected area) of $\mathbf{1}_{IMI}^{3H+} \bullet \mathbf{5}_{DopaMe2NH3+}^{-4H+}$.

Figure S18. 2D NMR HMQC spectrum ($CDCl_3$, 298 K) of $\mathbf{1}_{IMI}^{3H+} \bullet \mathbf{5}_{DopaMe2NH3+}^{-4H+}$.

Figure S19. ^{1}H NMR spectra ($CDCl_3$, 298 K) of (a) $\mathbf{3}_{IMI}^{3H+} \bullet \mathbf{4}_{PrNH3+}^{-3H+}$,**Pic**$^-$, (b) $\mathbf{3}_{IMI}^{3H+} \bullet \mathbf{4}_{PrNH3+}^{-4H+}$, (c) $\mathbf{3}_{IMI}^{3H+} \bullet \mathbf{2}_{PrNH3+}^{-3H+}$,**Pic**$^-$ and (d) $\mathbf{3}_{IMI}^{3H+} \bullet \mathbf{Cl}^- \bullet \mathbf{2}_{PrNH3+}^{-3H+}$.

Figure S20. ^{1}H NMR titration ($CDCl_3$, 298 K) of calix[6]hexa-acid **4** by $PrNH_2$.

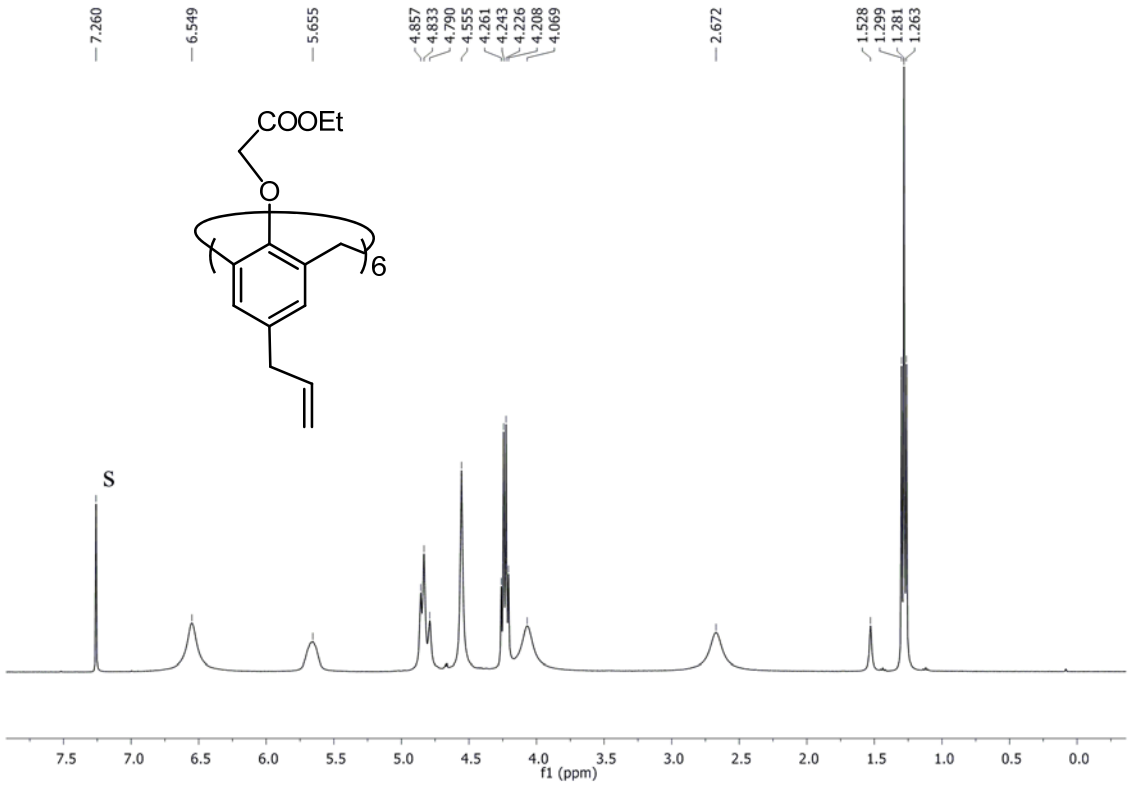

Figure S1. ^{1}H NMR spectrum ($CDCl_3$, 328 K, 400 MHz) of **7**; s = solvent.

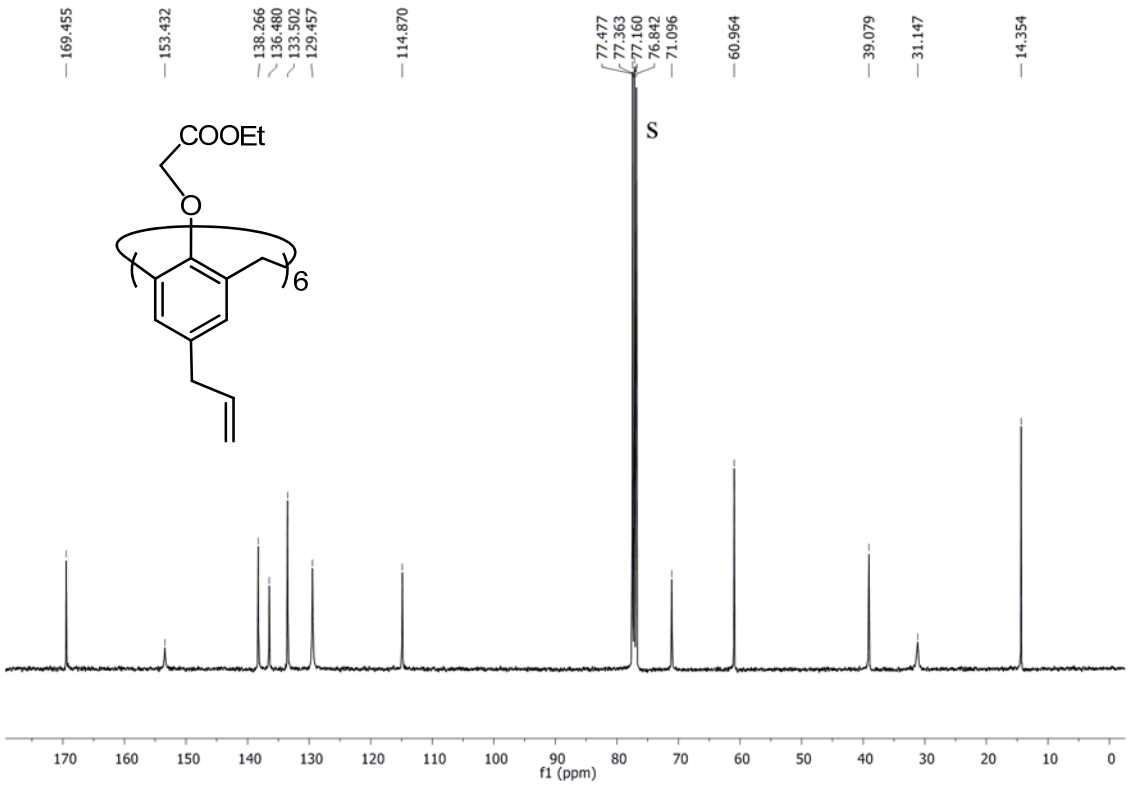

Figure S2. ^{13}C NMR spectrum ($CDCl_3$, 328 K, 100 MHz) of **7**; s = solvent.

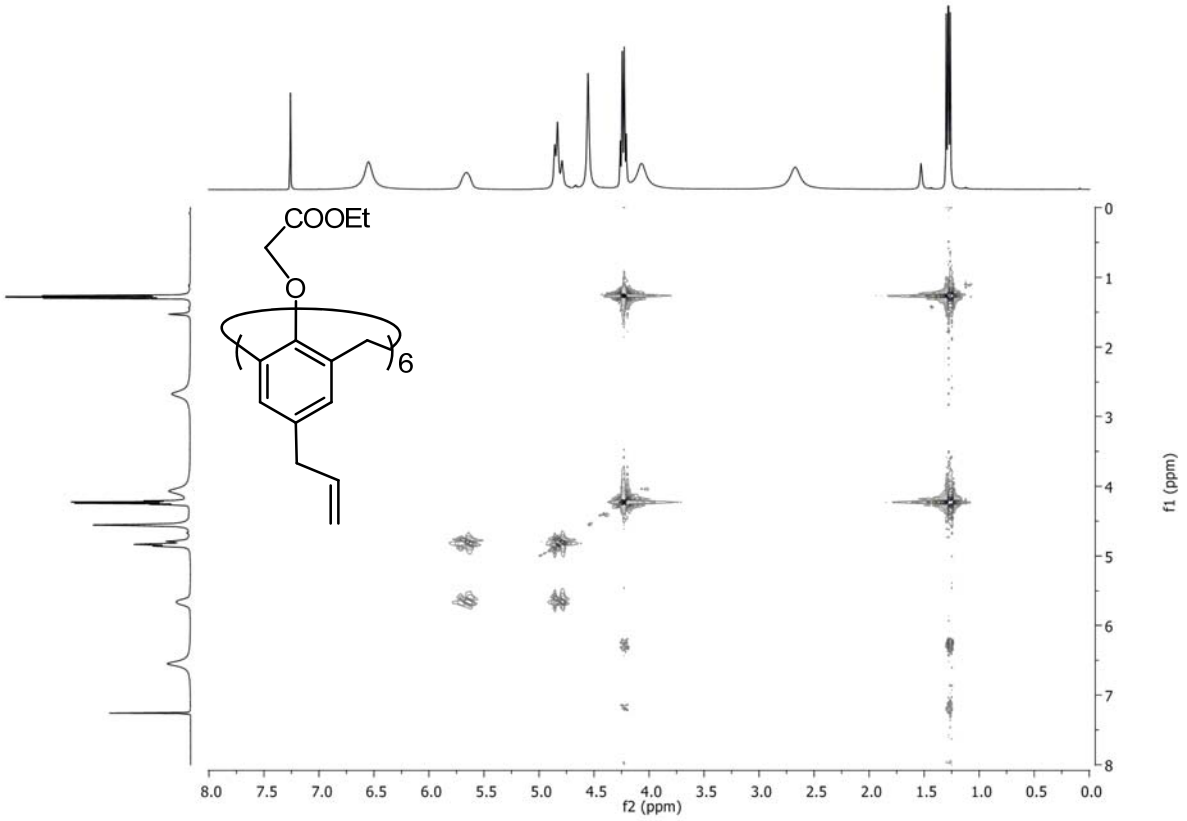

Figure S3. 2D NMR COSY spectrum ($CDCl_3$, 328 K) of **7**.

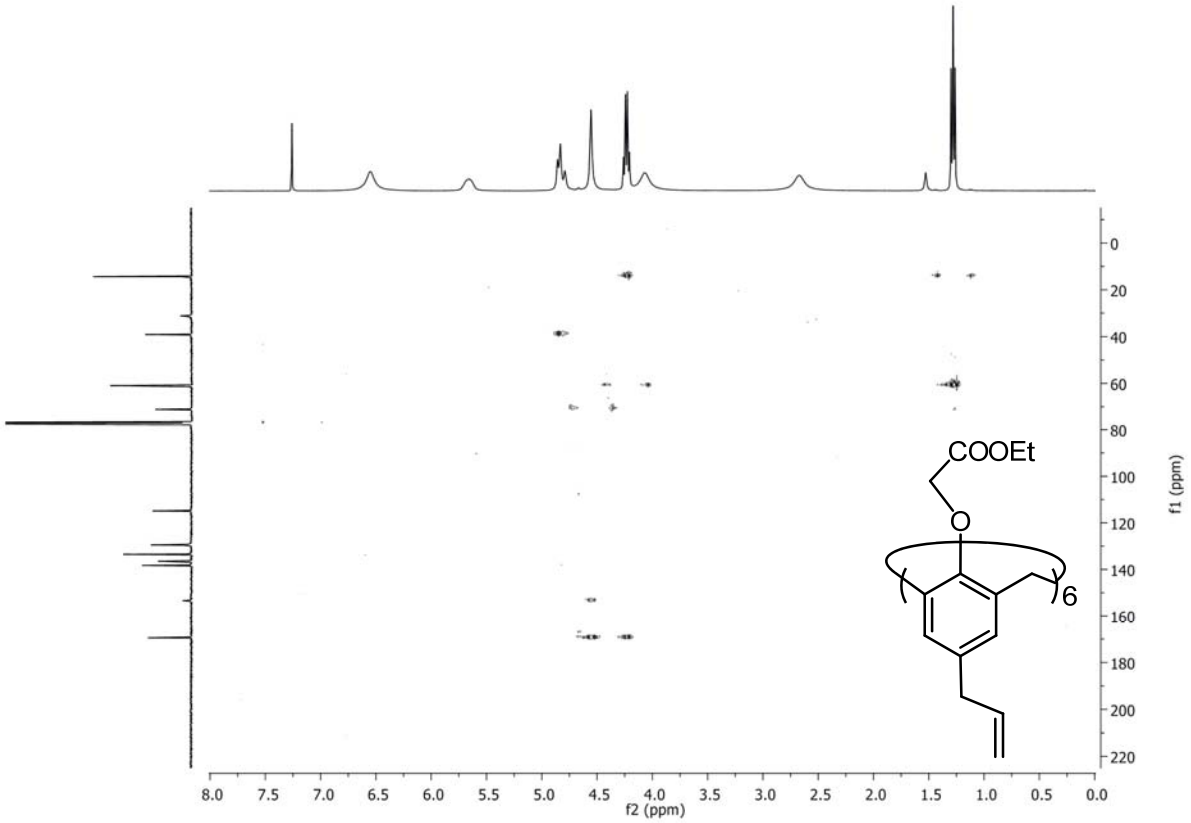

Figure S4. 2D NMR HMBC spectrum ($CDCl_3$, 328 K) of **7**.

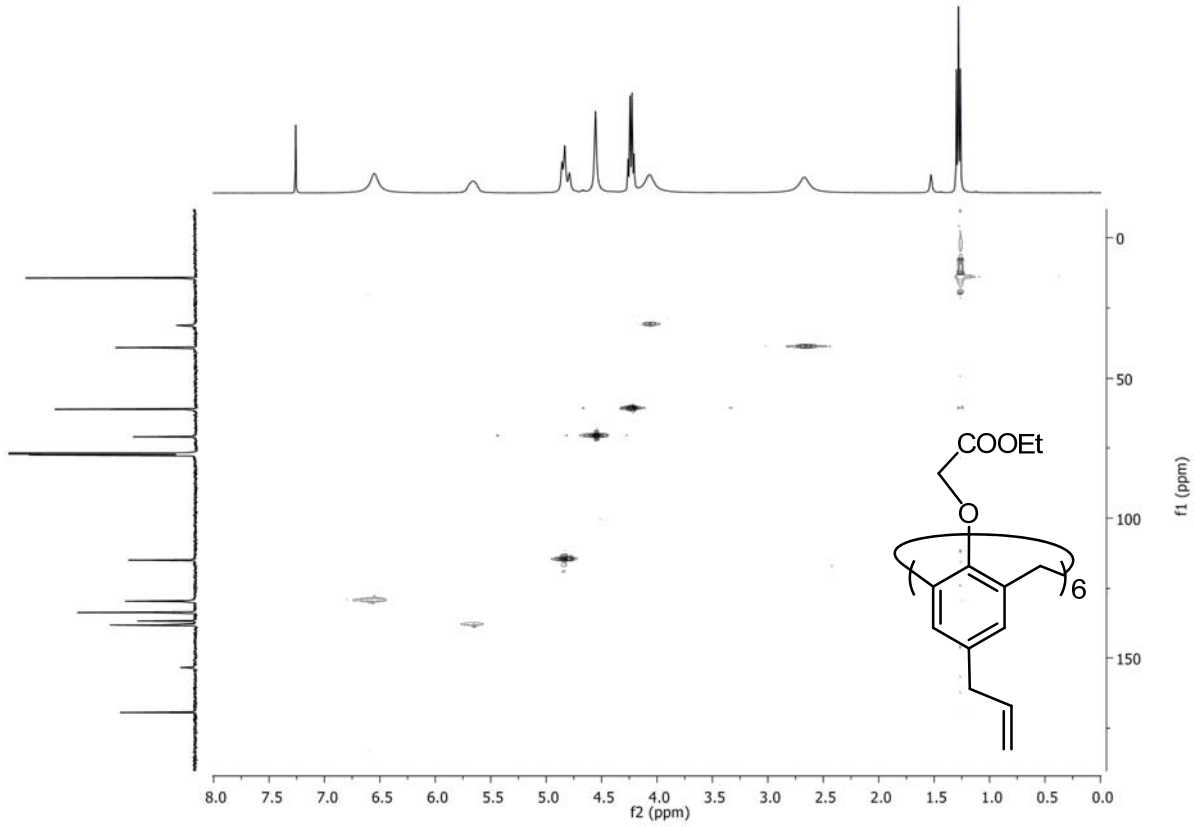

Figure S5. 2D NMR HSQC spectrum ($CDCl_3$, 328 K) of **7**.

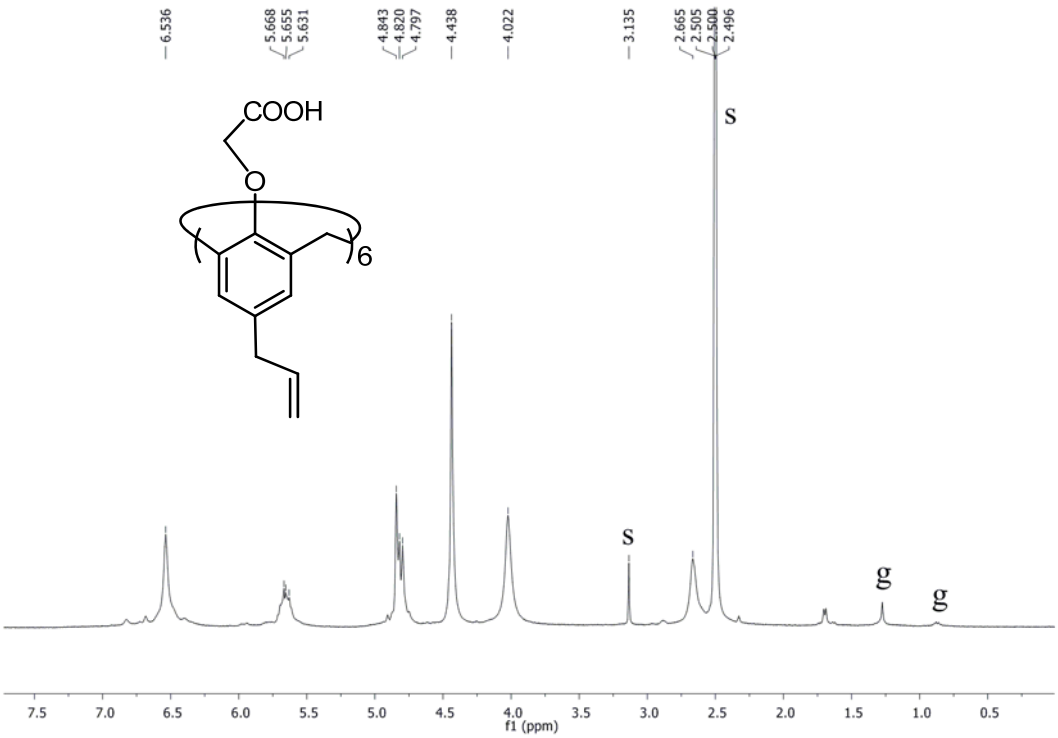

Figure S6. ^{1}H NMR spectrum (DMSO-d_6, 373 K, 400 MHz) of **8** (s = solvent, g = residual grease).

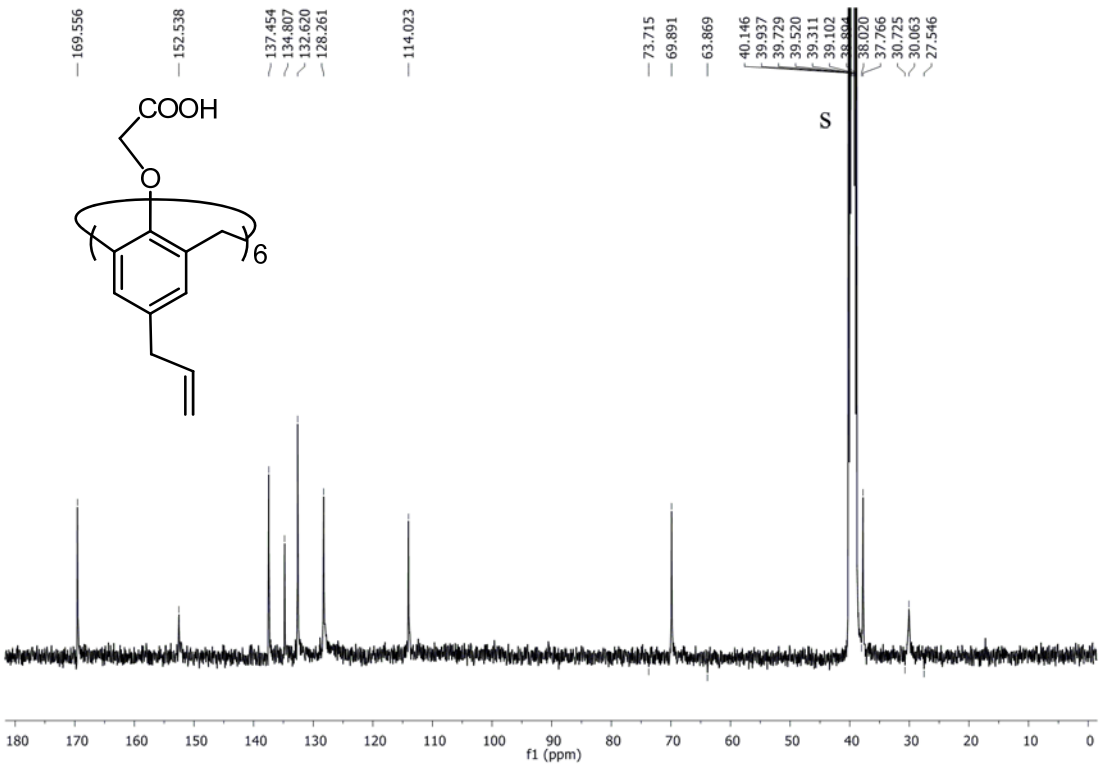

Figure S7. ^{13}C NMR spectrum (DMSO-d_6, 373 K, 100 MHz) of **8** (s = solvent).

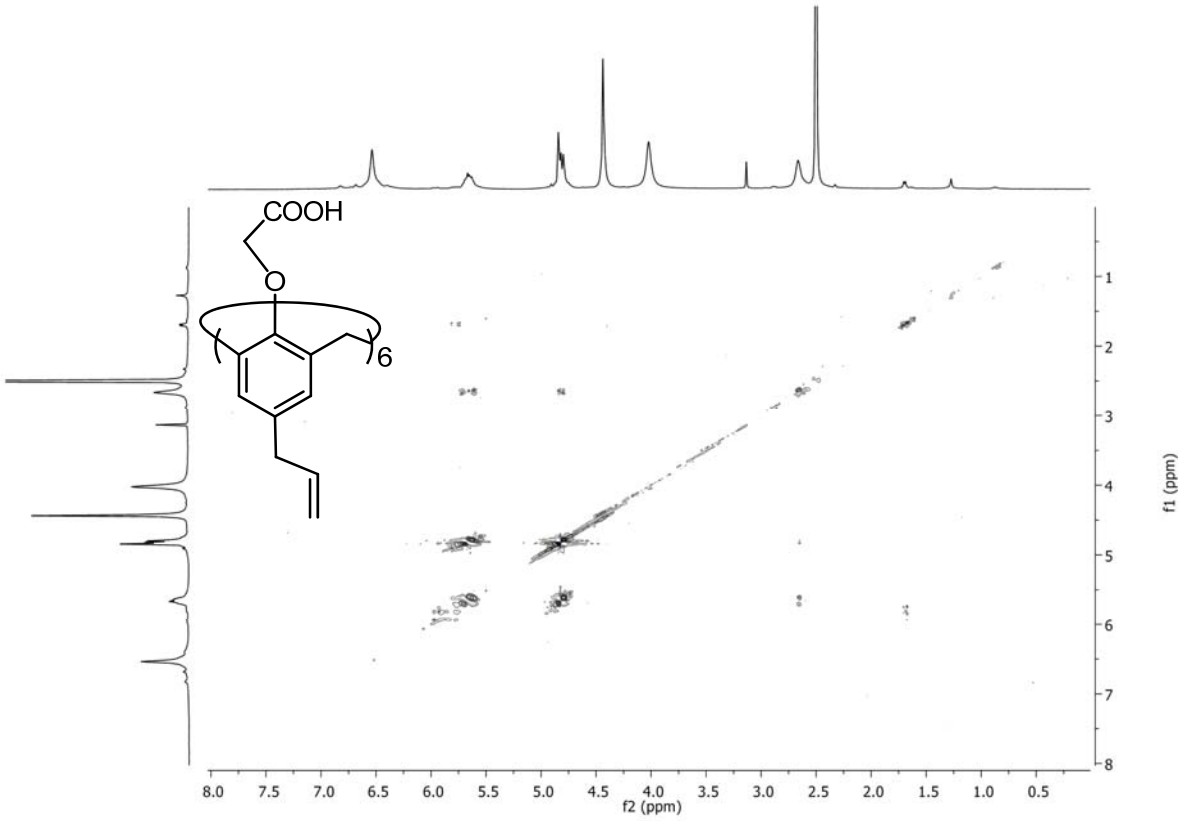

Figure S8. 2D NMR COSY spectrum (DMSO-d_6, 373 K) of **8**.

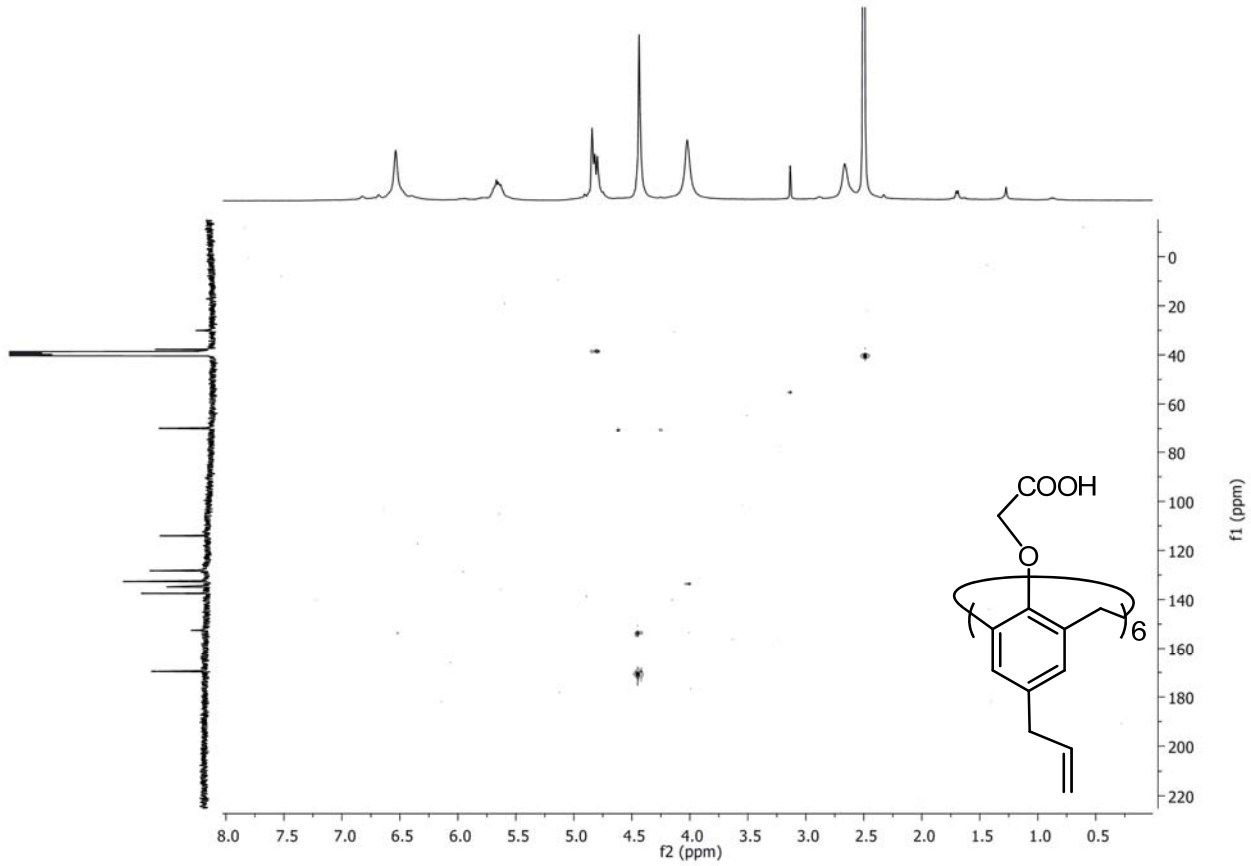

Figure S9. 2D NMR HMBC spectrum (DMSO-d_6, 373 K) of **8**.

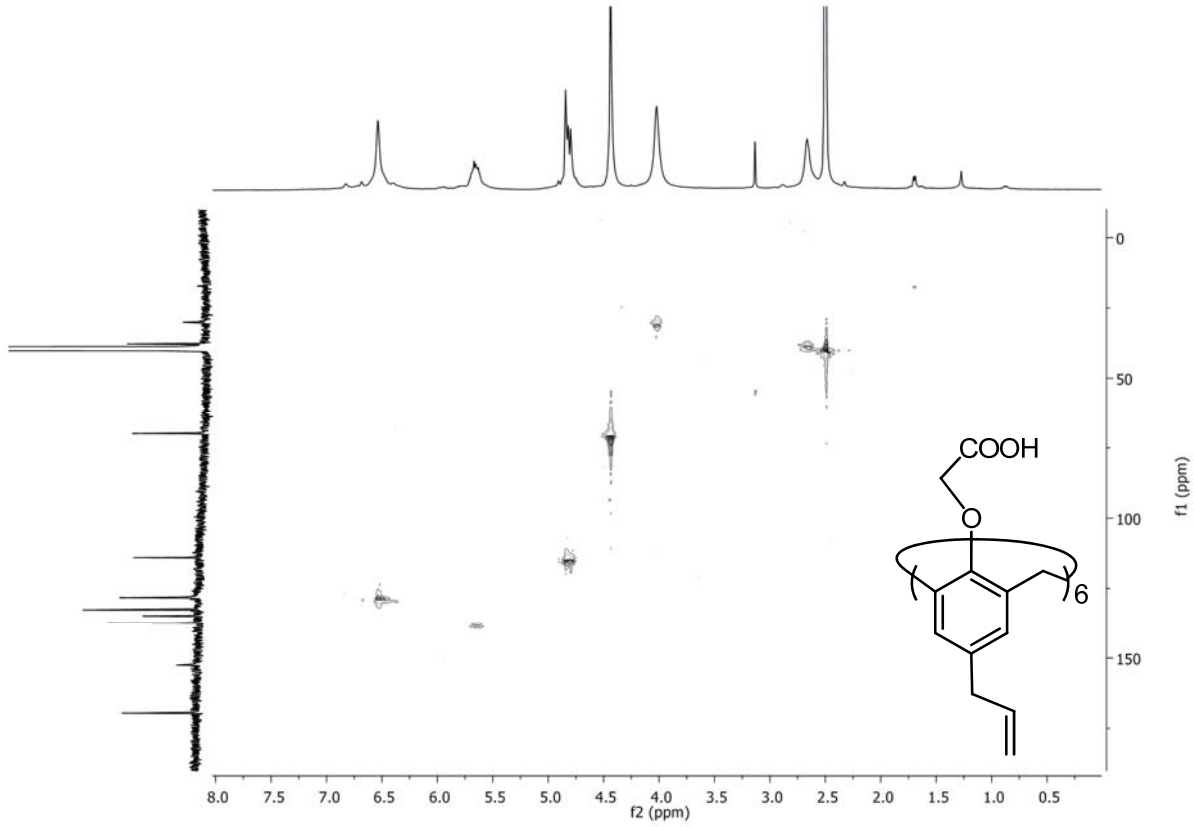

Figure S10. 2D NMR HSQC spectrum (DMSO-d_6, 373 K) of **8**.

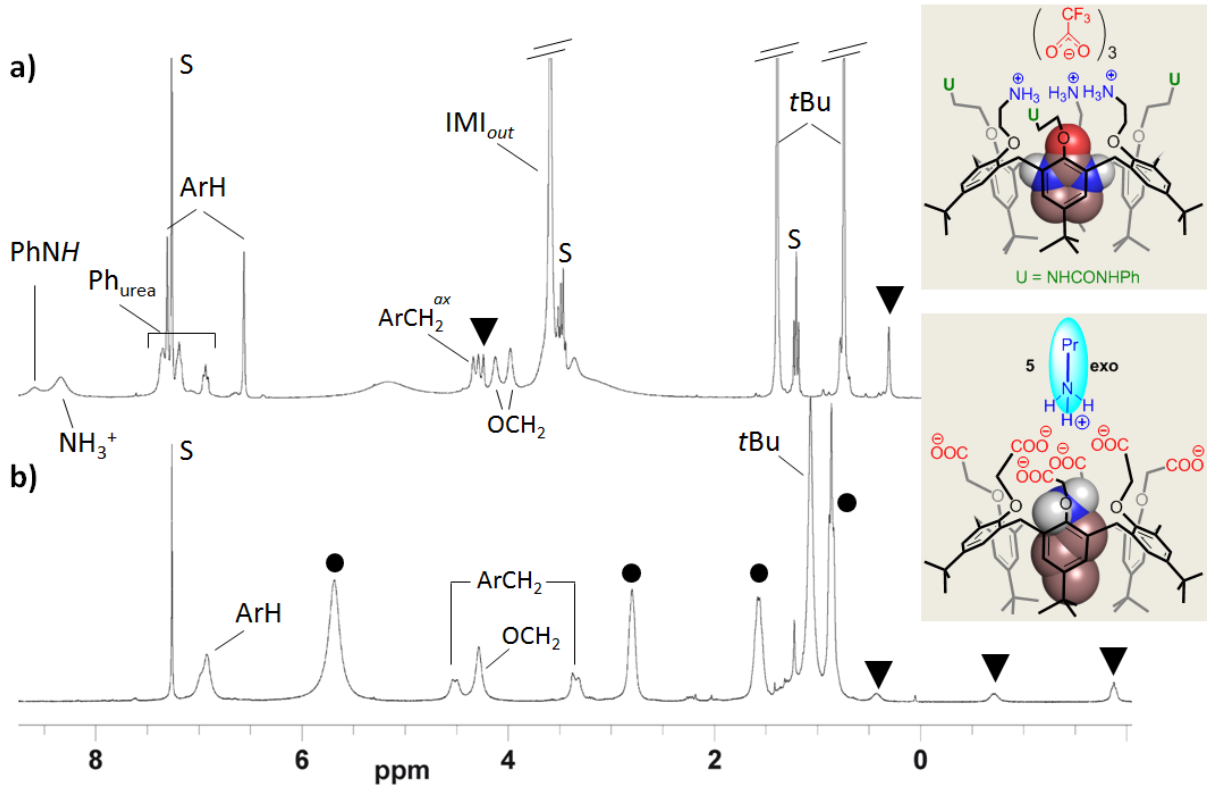

Figure S11. ^{1}H NMR spectra ($CDCl_3$, 298 K) of the host-guest complexes (a) $\mathbf{3}_{\boldsymbol{IMI}}^{\boldsymbol{3H+,3TFA-}}$ and (b) $\mathbf{4}_{\boldsymbol{PrNH3+}}^{\boldsymbol{-6H+,5PrNH3+}}$. ▼: IMI *in* or $PrNH_3^+$ *in*; •: $PrNH_2$ *out*; S = solvent.

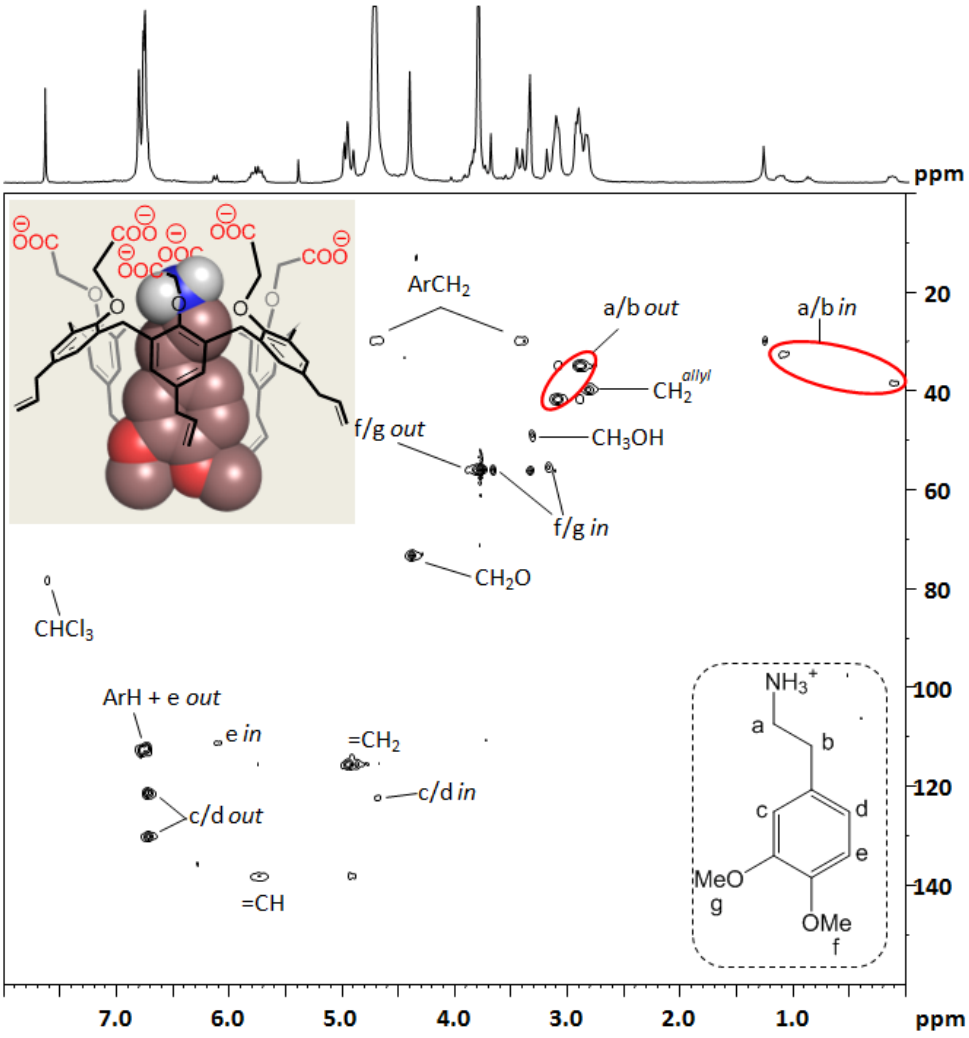

Figure S12. 2D NMR HMQC spectrum (2:1 $CD_3OD/CDCl_3$ solution, 298 K) of host-guest complex $\mathbf{8}^{-6H+,5DopaMe2NH3+}_{DopaMe2NH3+}$.

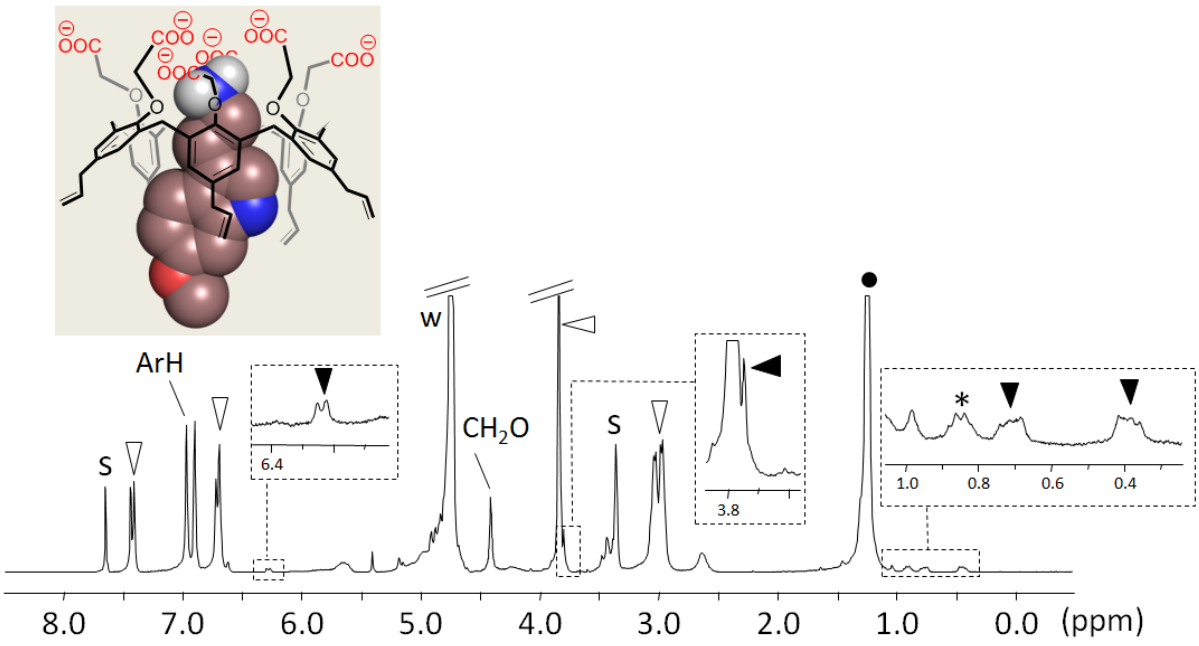

Figure S13. ^{1}H NMR spectra (2:1 $CD_3OD/CDCl_3$ solution, 298 K) of host-guest complex $\mathbf{8}_{TryptMeNH3+}^{-6H+,5tBuNH3+}$. S = solvent; w = water; ▼: *TryptMe in*; Δ: *TryptMe out* (16 equiv.); •: *t*BuNH$_2$ (20 equiv.); *: residual grease.

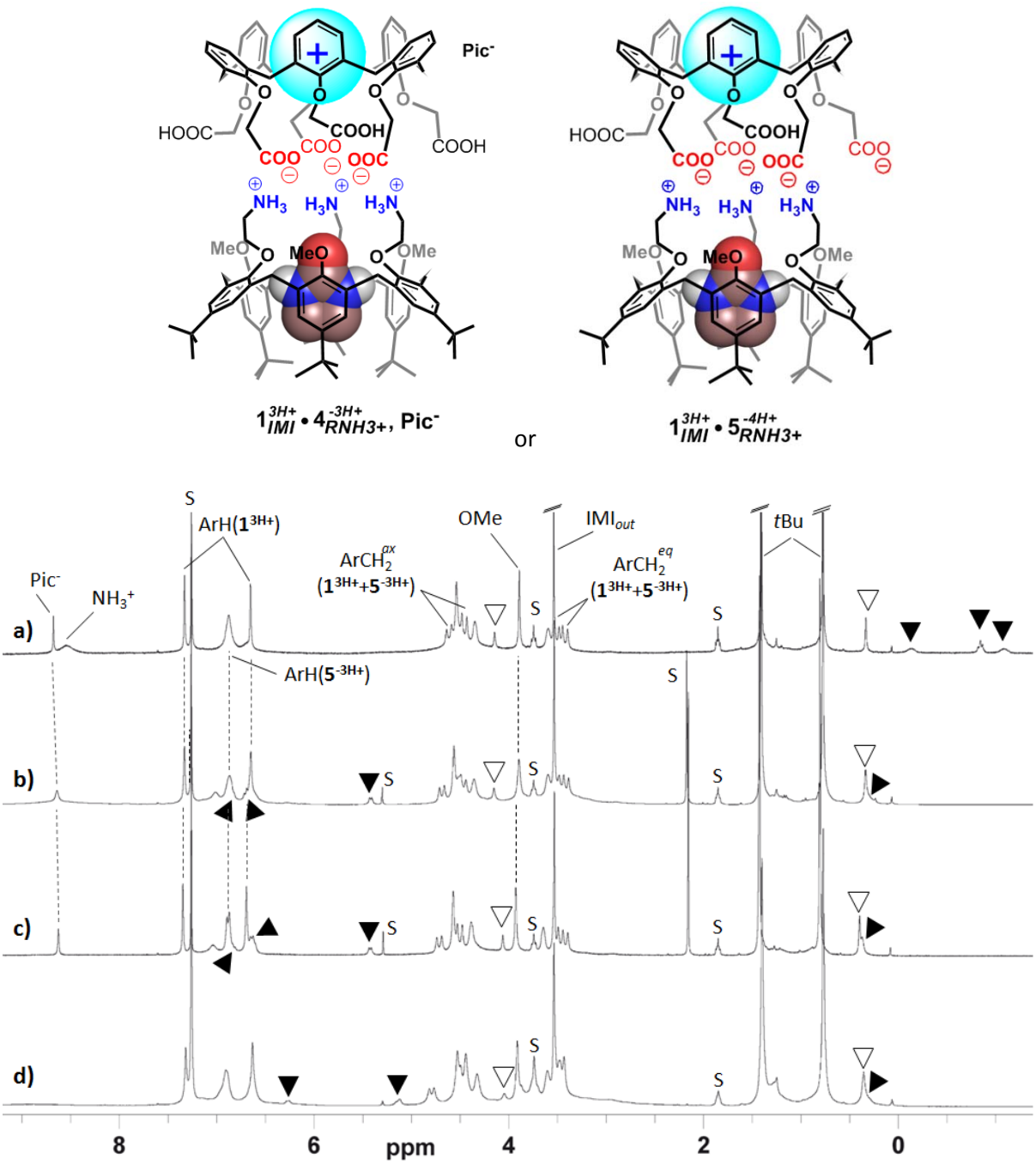

Figure S14. ^{1}H NMR spectra ($CDCl_3$) of (a) the assembly $\mathbf{1^{3H+}_{IMI} \bullet 5^{-3H+}_{PrNH3+}}$,**Pic**⁻ at 298 K, of the assembly $\mathbf{1^{3H+}_{IMI} \bullet 5^{-3H+}_{PhCH2CH2NH3+}}$,**Pic**⁻ at 298 K (b) and at 330 K (c), and of the assembly $\mathbf{1^{3H+}_{IMI} \bullet 5^{-4H+}_{DopaMe2NH3+}}$ at 298 K. S = solvent; Δ: IMI *in*; ▼: ammonium *in*.

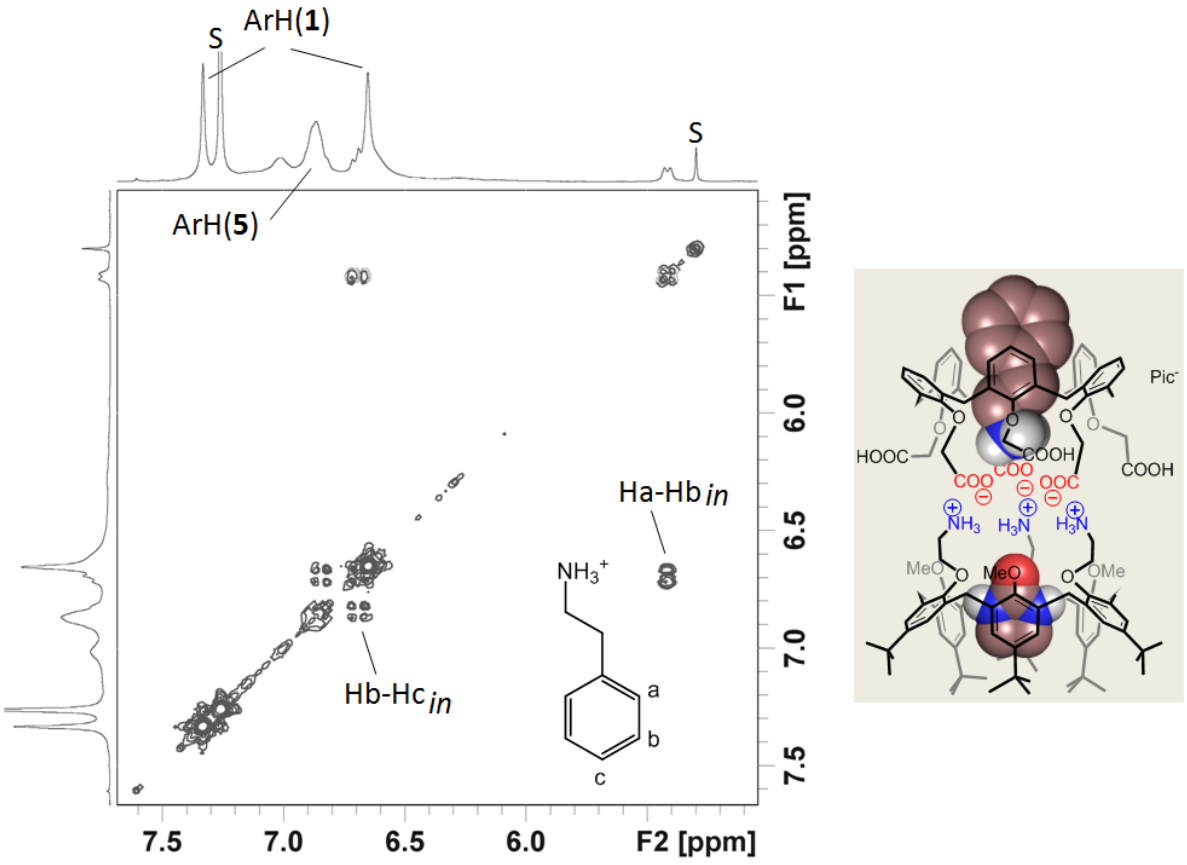

Figure S15. 2D NMR COSY spectrum ($CDCl_3$, 298 K, selected area) of $\mathbf{1}_{IMI}^{3H+}$ • $\mathbf{5}_{PhCH2CH2NH3+}^{-3H+}$,$Pic^-$. S = solvent.

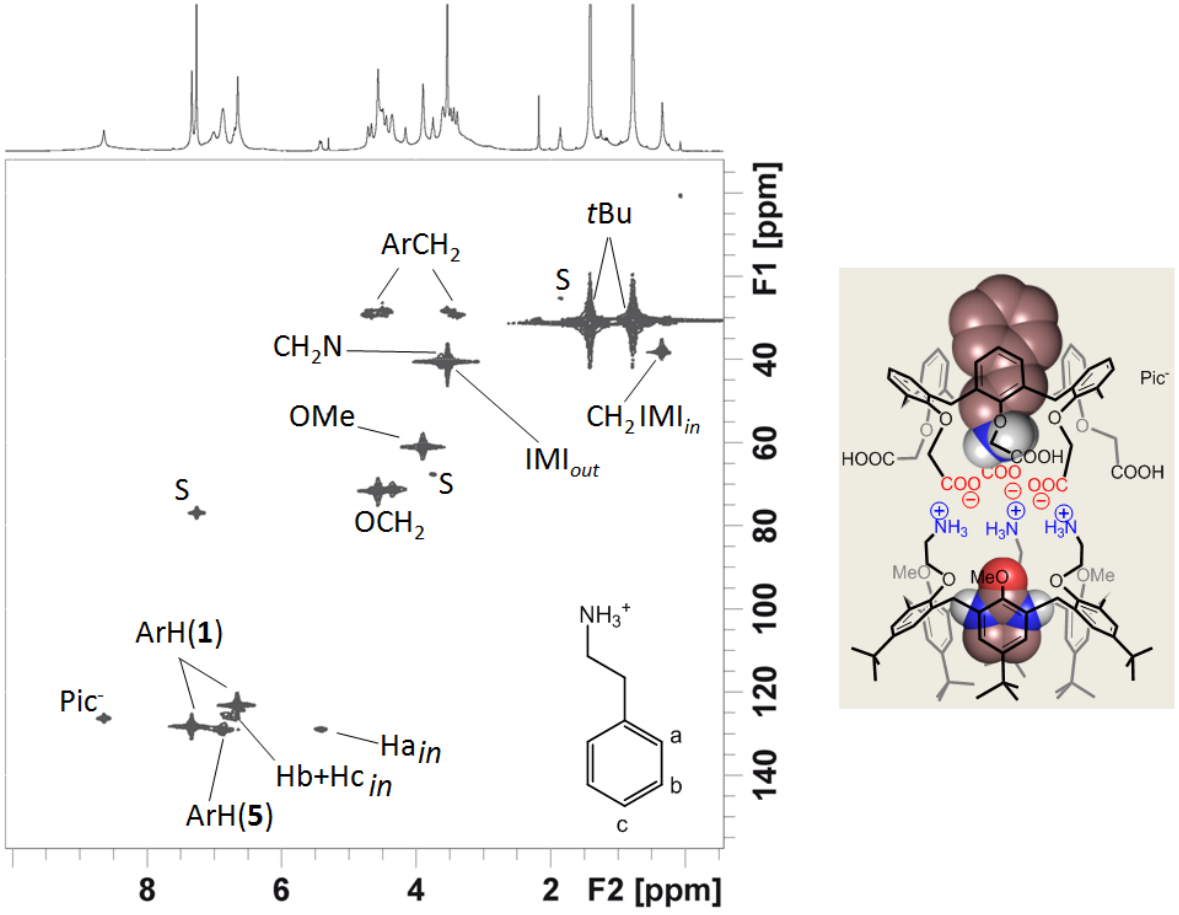

Figure S16. 2D NMR HMQC spectrum ($CDCl_3$, 298 K) of $\mathbf{1}_{IMI}^{3H+}$ • $\mathbf{5}_{PhCH2CH2NH3+}^{-3H+}$,$Pic^-$. S = solvent.

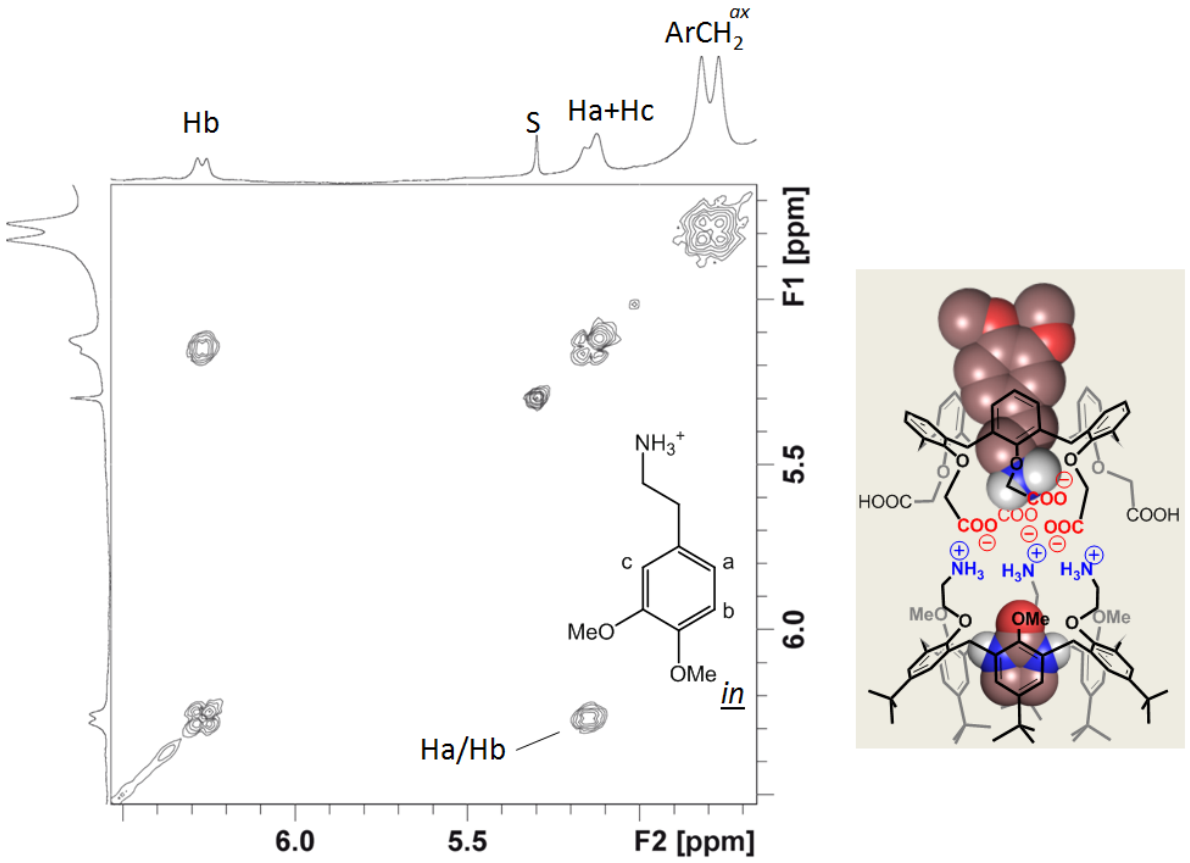

Figure S17. 2D NMR COSY spectrum ($CDCl_3$, 298 K, selected area) of $\mathbf{1}_{IMI}^{3H+} \bullet \mathbf{5}_{DopaMe2NH3+}^{-4H+}$. S = solvent.

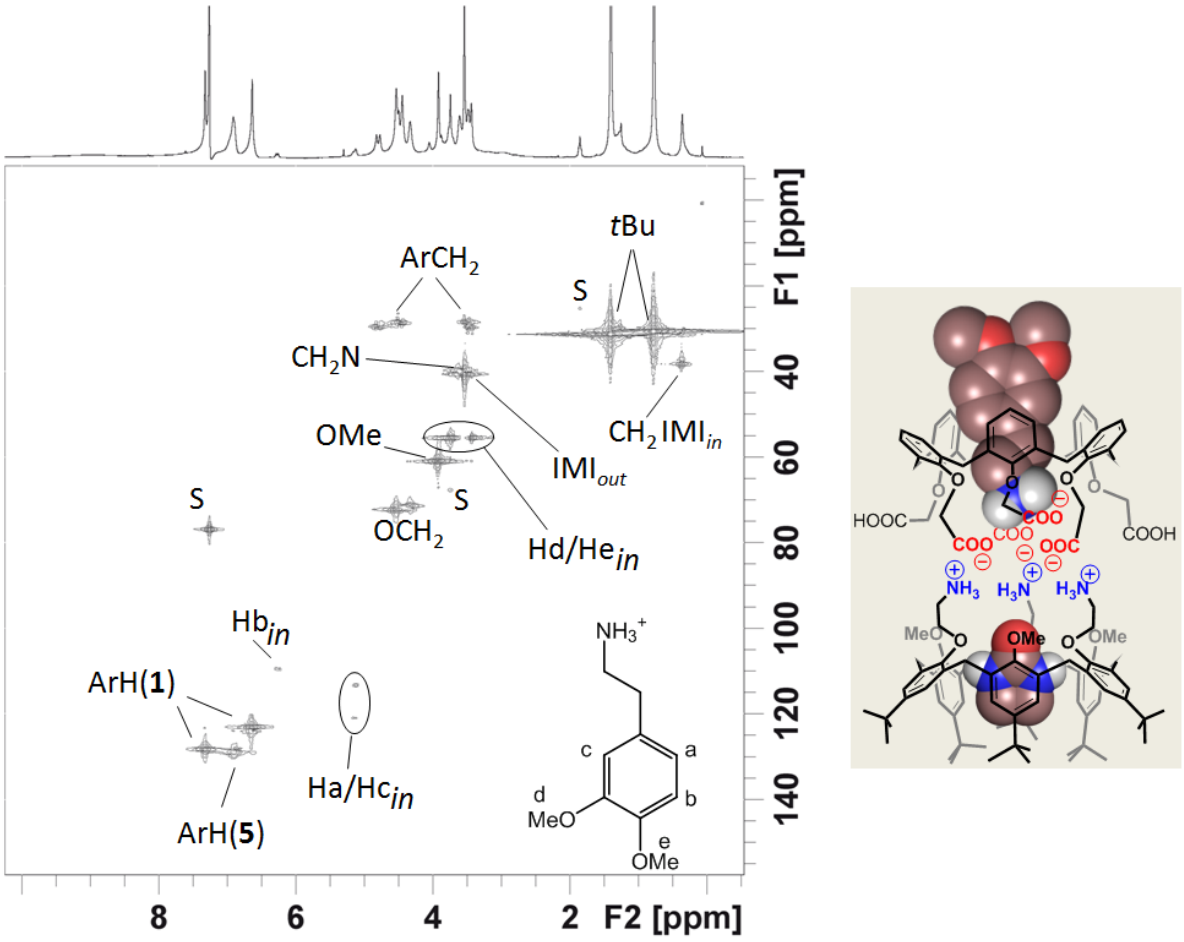

Figure S18. 2D NMR HMQC spectrum ($CDCl_3$, 298 K) of $\mathbf{1}_{IMI}^{3H+}$ • $\mathbf{5}_{DopaMe2NH3+}^{-4H+}$. S = solvent.

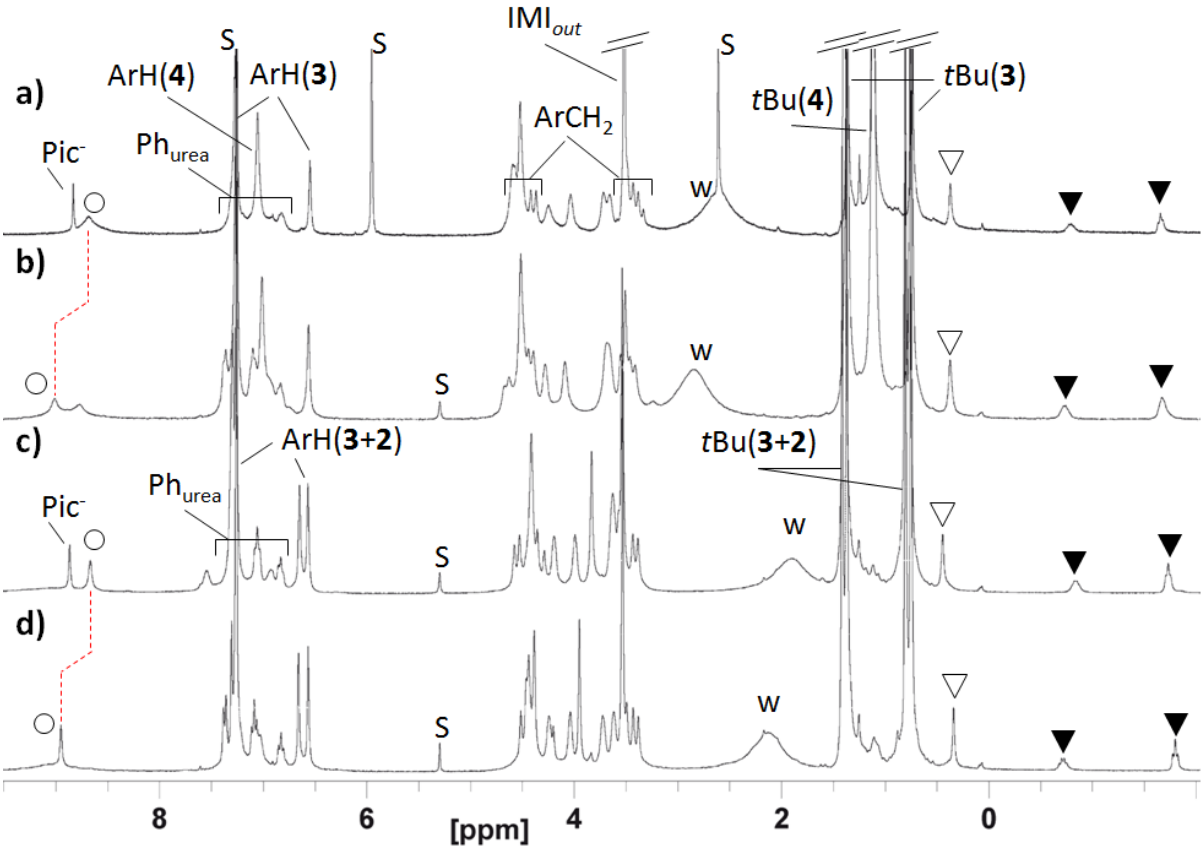

Figure S19. ^{1}H NMR spectra ($CDCl_3$, 298 K) of (a) $\mathbf{3}_{IMI}^{3H+} \bullet \mathbf{4}_{PrNH3+}^{-3H+}$,Pic$^-$, (b) $\mathbf{3}_{IMI}^{3H+} \bullet \mathbf{4}_{PrNH3+}^{-4H+}$, (c) $\mathbf{3}_{IMI}^{3H+} \bullet \mathbf{2}_{PrNH3+}^{-3H+}$,Pic$^-$ and (d) $\mathbf{3}_{IMI}^{3H+} \bullet \mathbf{Cl}^- \bullet \mathbf{2}_{PrNH3+}^{-3H+}$. S = solvent; W = water; Δ: IMI *in*; ▼: $PrNH_3^+$ *in*; O: CON*H*Ph protons.

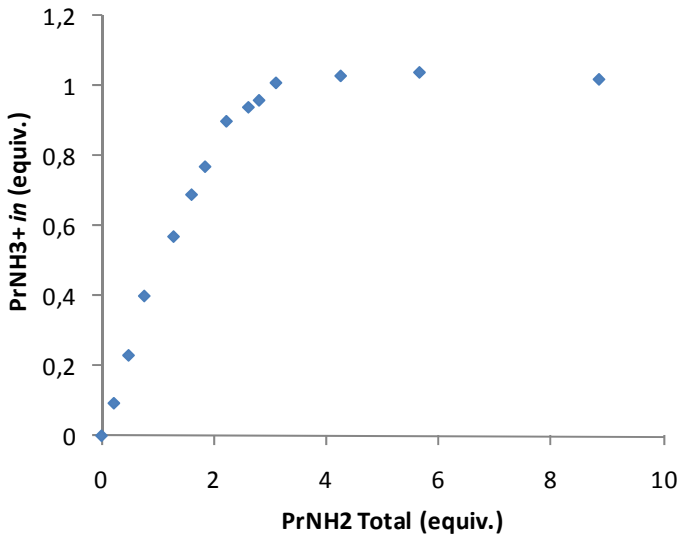

Figure S20. ^{1}H NMR titration of calix[6]hexa-acid **4** by $PrNH_2$ ($CDCl_3$, 298 K), showing the quantitative inclusion of the propylammonium ion upon addition of 3 equiv. of $PrNH_2$.